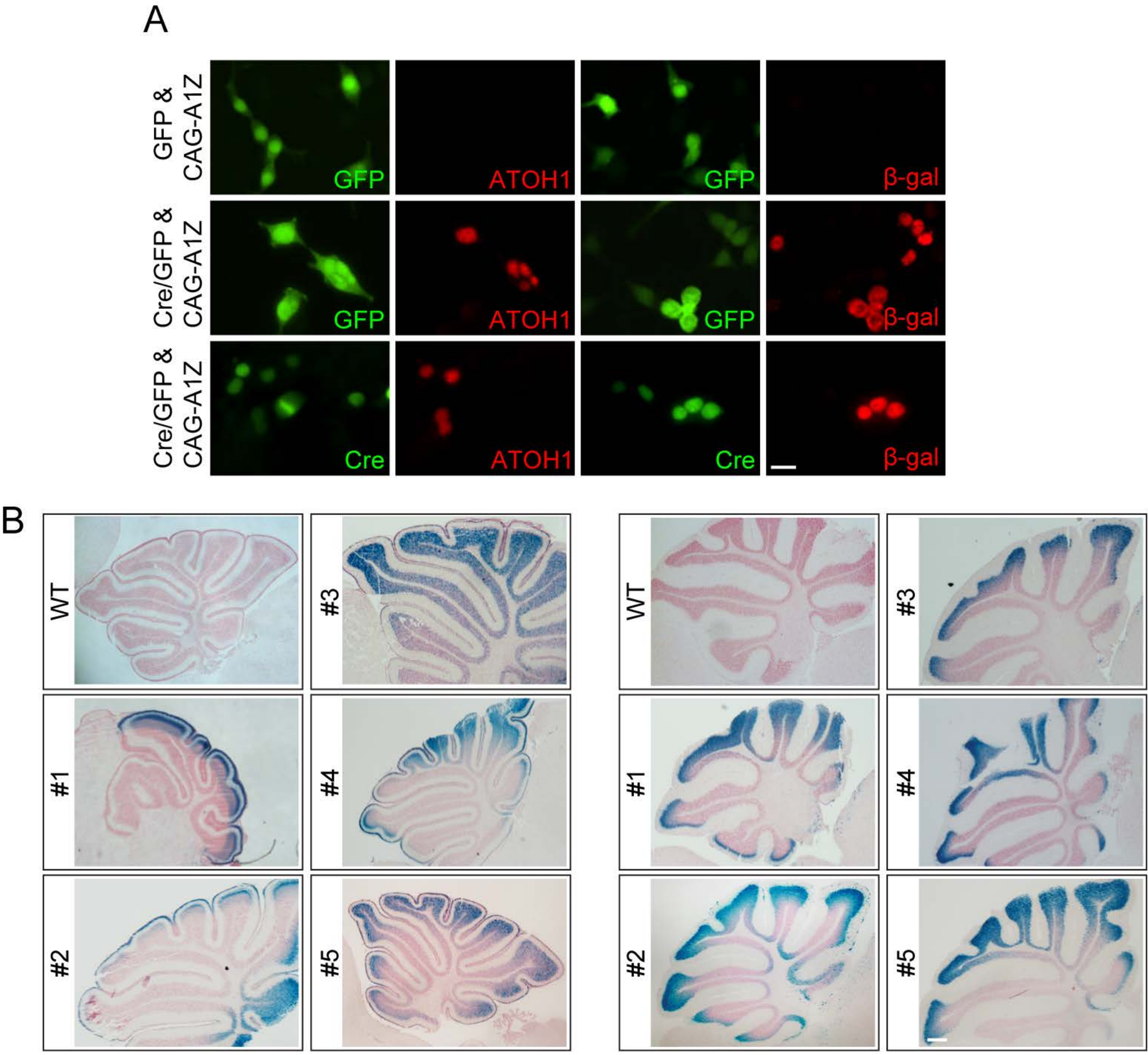

Supplemental figure 1

Supplemental Figure 1 Analysis of gene expression in *CAG-A1Z* transgenic mice. (A) Representative images of *Atoh1* transgene expression in human embryonic kidney (HEK)-293 cells transfected with *CAG-A1Z* construct along with vectors expressing Cre and GFP or GFP only. Notice that ATOH1 (red) and β-galactosidase (red) are expressed in cells co-transfected with vector expressing Cre/GFP (green), but not in cells co-transfected with control GFP vector. Scale bar, 5 μm. (B) *Math1-cre;CAG-A1Z* mice (lines #1, #2), *Atoh1-creER;CAG-A1Z* mice (lines #3, #4, #5) treated with tamoxifen from day P1 to P3, and wild type (WT) animals are shown. At P11 (left panel) and P23 (right panel), brains from these animals were processed for whole-mount X-Gal staining. Representative images of the cerebellum stained with X-Gal are shown with nuclear fast red as counterstaining. Lack of LacZ expression in deeper region within cerebellar cortex likely arose from insufficient penetration of staining solution. Scale bar, 250 μm.

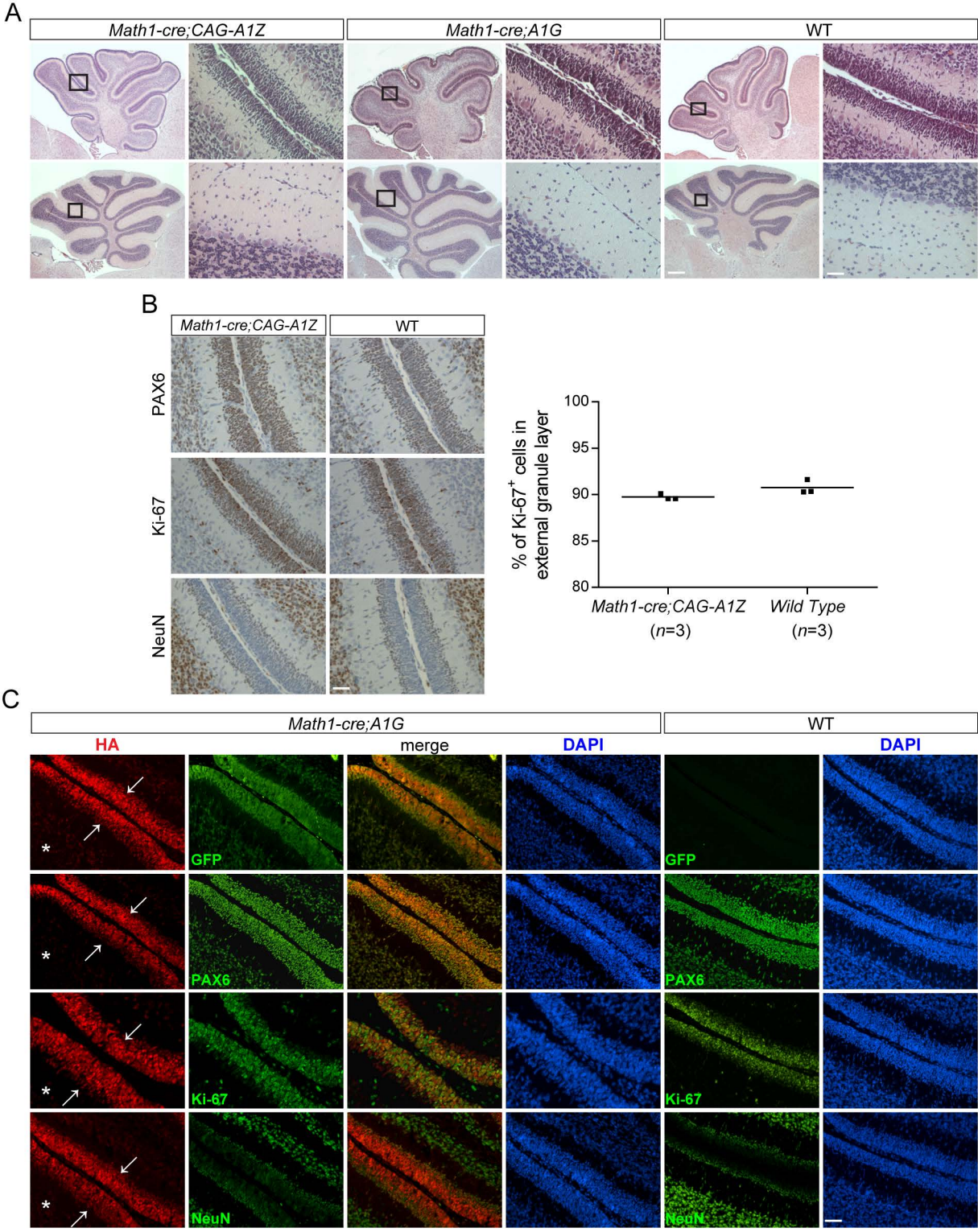

Supplemental figure 2

Supplemental Figure 2 Normal cerebellar development in *Atoh1* transgenic animals. (A) H&E staining of cerebella from *Math1-cre;CAG-A1Z* (*CAG-A1Z* line #2), *Math1-cre;A1G*, and wild type (WT) mice at P7 (top row) and P21 (bottom row). Boxed regions in representative images are shown in higher magnification (right column of each panel). Scale bars, 250 μm (left column of each panel) and 25 μm (right column of each panel). (B) The expression of PAX6, Ki-67, and NeuN is shown in the cerebellum of *Math1-cre;CAG-A1Z* mice shown in (A). Scale bar, 25 μm. Quantification of the percentage of Ki-67^{+} GNPs in the external granule layer of cerebellum in *Math1- cre;CAGA1Z* and wild type mice at P7 is shown (*n*=3 cerebella from 3 animals of each genotype, data from a single experiment are shown; mean, two-tailed unpaired t-test). (C) Analysis of *Atoh1-HA* transgene (ATOH1-HA and eGFP) and gene expression in the cerebellum of *Math1-cre;A1G* and wild type (WT) mice shown in (A). HA staining (red) marks *Atoh1*$^{+}$ progenitors (arrows) and differentiated granule neurons (*) that express the transgene. The expression of PAX6, Ki-67, NeuN and eGFP (all green) is shown. DAPI staining (blue) labels nuclei. Scale bar, 25 μm.

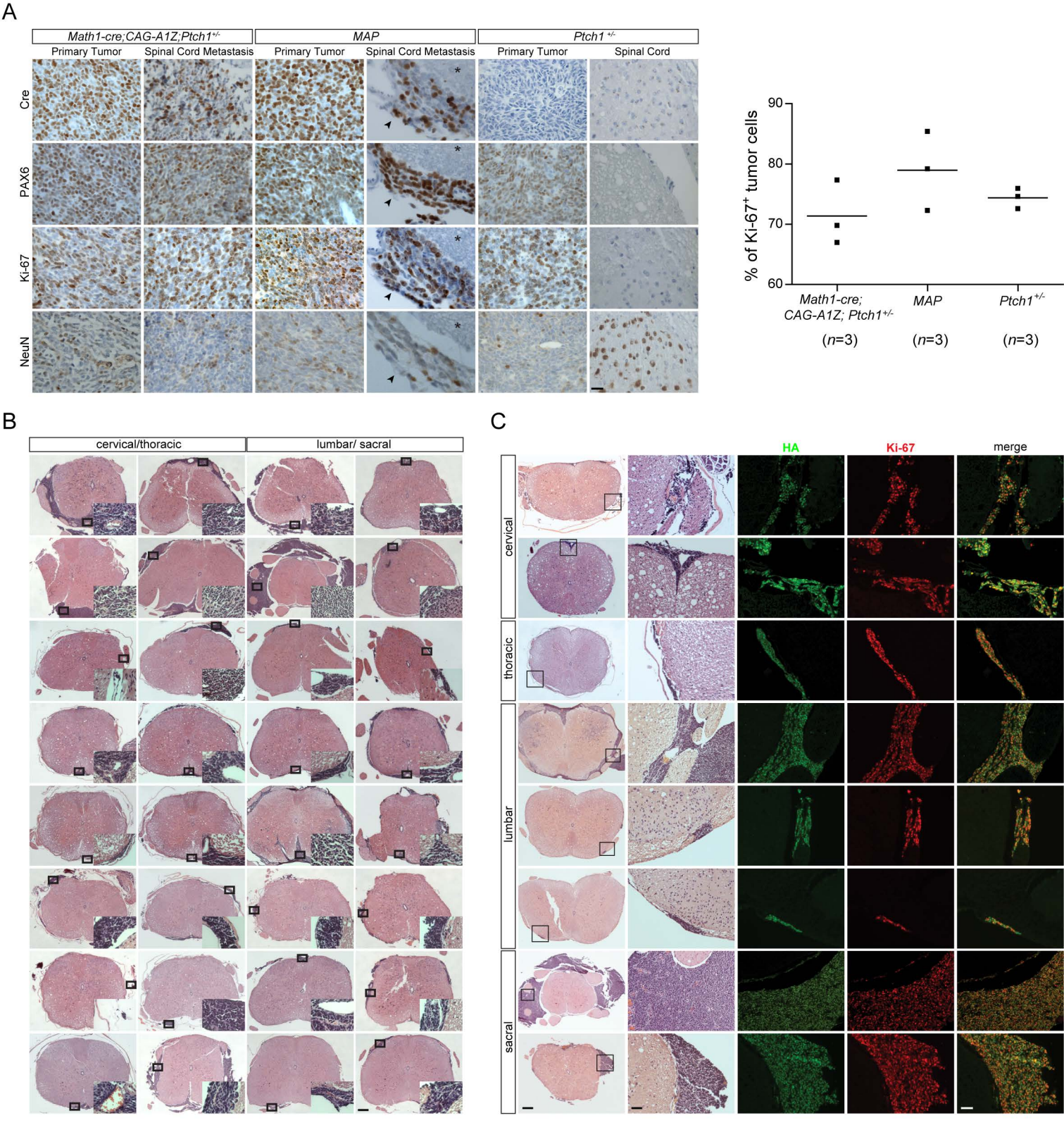

Supplemental figure 3

Supplemental Figure 3 *Atoh1* over-expression enhances MB development and metastasis along the spinal cord in *Ptch1*$^{+/-}$ mice. (A) Expression of the Cre, PAX6, Ki-67, and NeuN is shown in primary and metastatic tumor (arrowheads) in the spinal cord of representative *Math1Cre;CAG-A1Z;Ptch1*$^{+/-}$*; MAP* and *Ptch1*$^{+/-}$ mice. Scale bar, 12.5 μm. Quantification of the percentage of Ki-67^{+} tumor cells in MB from *Math1Cre;CAG-A1Z;Ptch1*$^{+/-}$, *MAP* and *Ptch1*$^{+/-}$ mice (*n*=3 tumors from 3 animals for each genotype, data from a single experiment are shown; mean, one-way ANOVA). (B) H&E staining is shown for metastatic tumor at different levels of the spinal cord in *MAP* mice. Boxed regions in representative images are magnified in inset pictures. Scale bar, 250 μm. (C) Left 2 columns: H&E staining is shown for metastatic tumor at different levels of the spinal cord in *MAP* mice. Boxed regions in representative images are magnified in the column to the right. Scale bars, 250 μm (left column) and 25 μm (right column). Right 3 columns: representative images of ATOH1-HA transgene (green) and Ki-67 (red) expression are shown in metastatic tumor displayed in the left two columns. Scale bar, 25 μm.

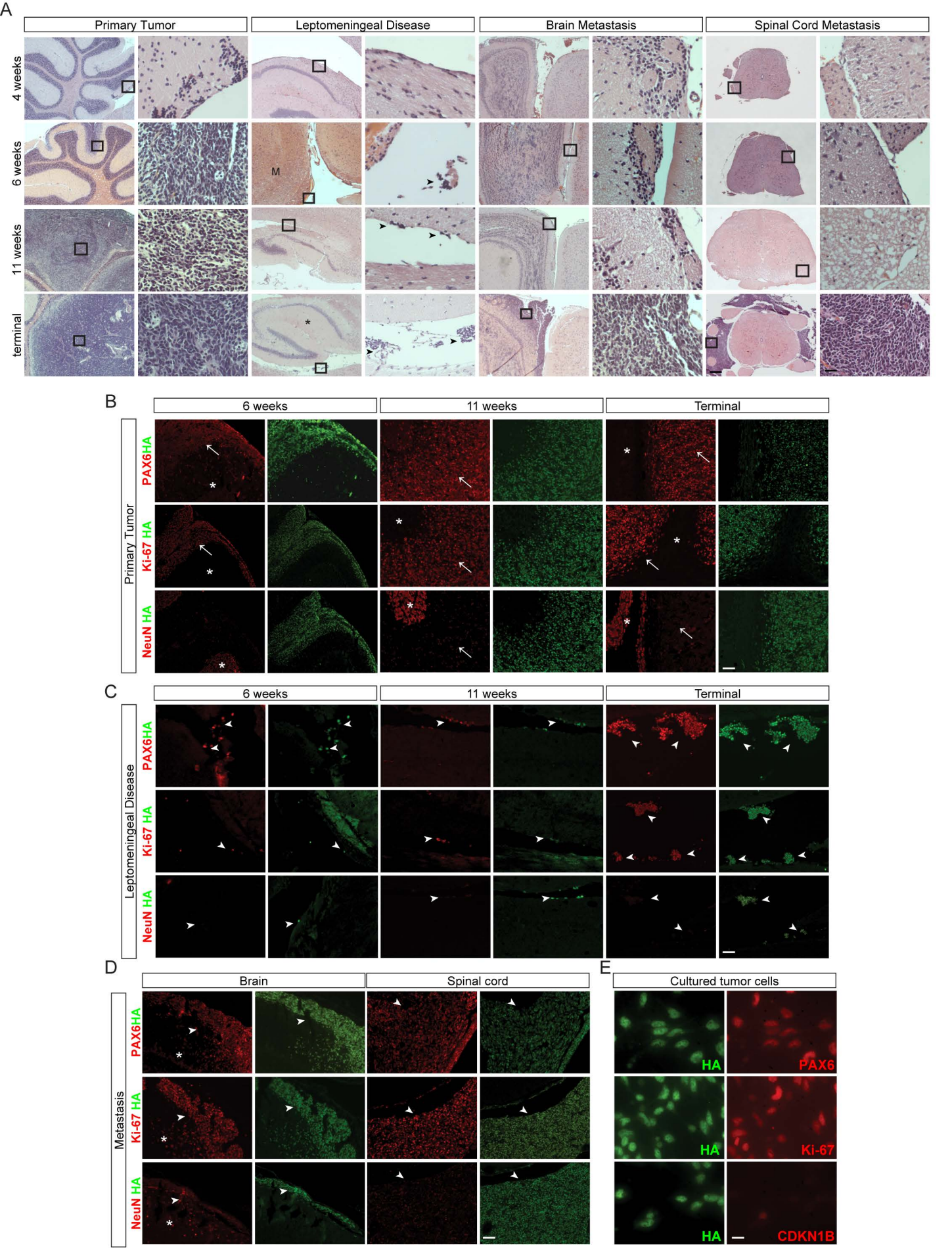

Supplemental figure 4

Supplemental Figure 4 ATOH1-driven MB development and metastasis. (A) H&E staining is shown for primary tumor in the cerebellum, disseminating tumor cells in CSF, and metastatic tumor in the brain and spinal cord from 4, 6, 11-week old, and terminally ill *MAP* mice. Boxed regions in representative images of primary tumor, disseminating tumor cells (arrowheads) adjacent to midbrain (M) and hippocampus (*), and metastatic growth in the brain and spinal cord are magnified in the column to the right in each panel. Scale bars, 250 μm (left column of each panel) and 25 μm (right column of each panel). (B-D) Expression of *Atoh1-HA* transgene (HA, green), PAX6 (red), Ki-67 (red), and NeuN (red) is shown in primary tumor (arrows, B), disseminating tumor cells from representative 6-, 11-week old, and terminally ill *MAP* mice (arrowheads, C), and representative metastatic tumor in the brain and spinal cord (arrowheads, D). Asterisks (*) mark the cerebellum and brain. Scale bars, 25 μm. (E) Representative images *Atoh1-HA* transgene (HA, green), PAX6, Ki-67, and CDKN1B (all red) expression in cultured tumor cells. Scale bar, 5 μm.

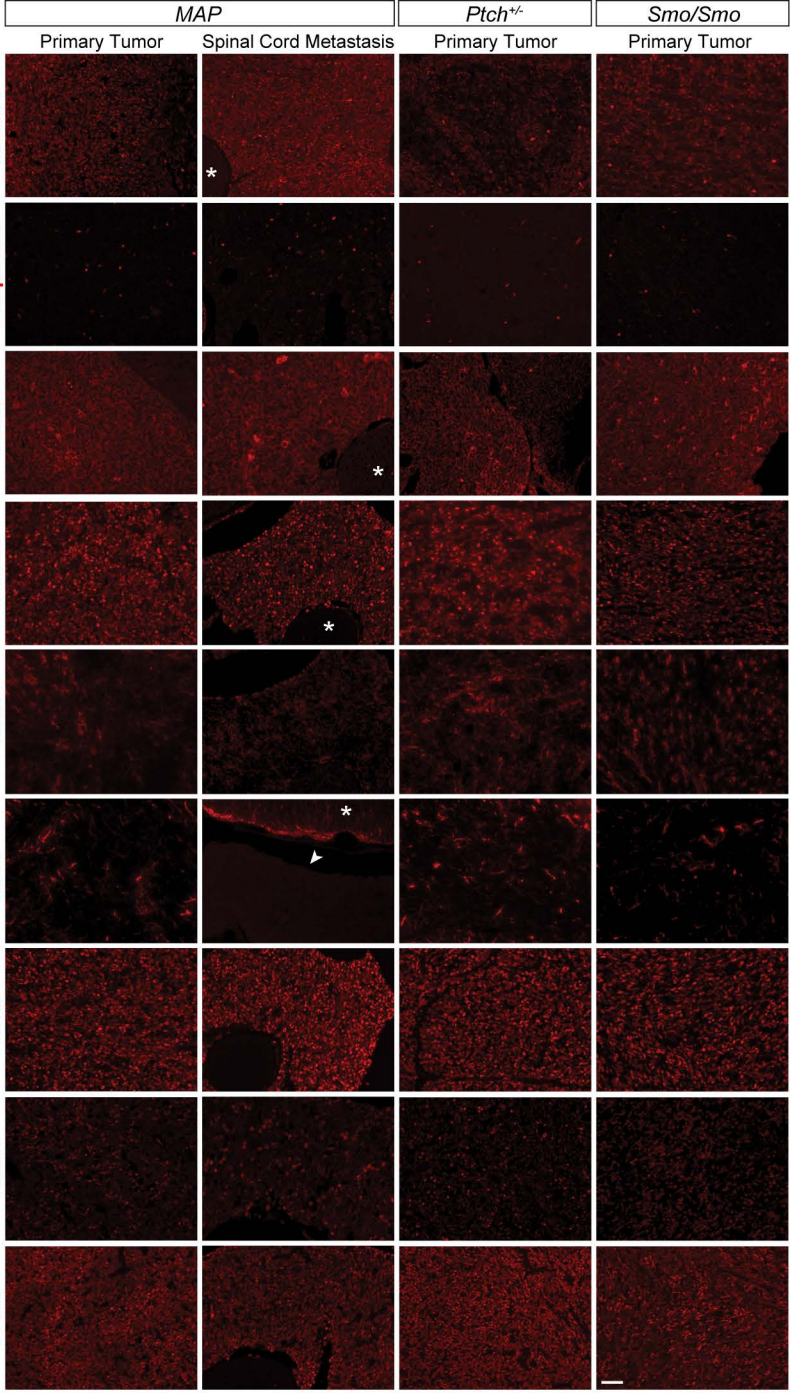

Supplemental figure 5

Supplemental Figure 5 Analysis of gene expression in SHH MB from different mouse strains. Representative images of the expression of ATOH1 (red), Cleaved caspase 3, Pyruvate Kinase M2 (PKM2, red), cyclin D1(CCND1, red), Neuron-specific class III beta-tubulin (TUJ1, red), Glial fibrillary acidic protein (GFAP, red), Ki-67 (red), NeuN (red), and PAX6 (red) are shown in primary and metastatic tumor (arrowhead) in the spinal cord (*) from *MAP* mice, and tumors from *Ptch1*$^{+/-}$ and *Smo/Smo* mice. Scale bar: 25 μm.

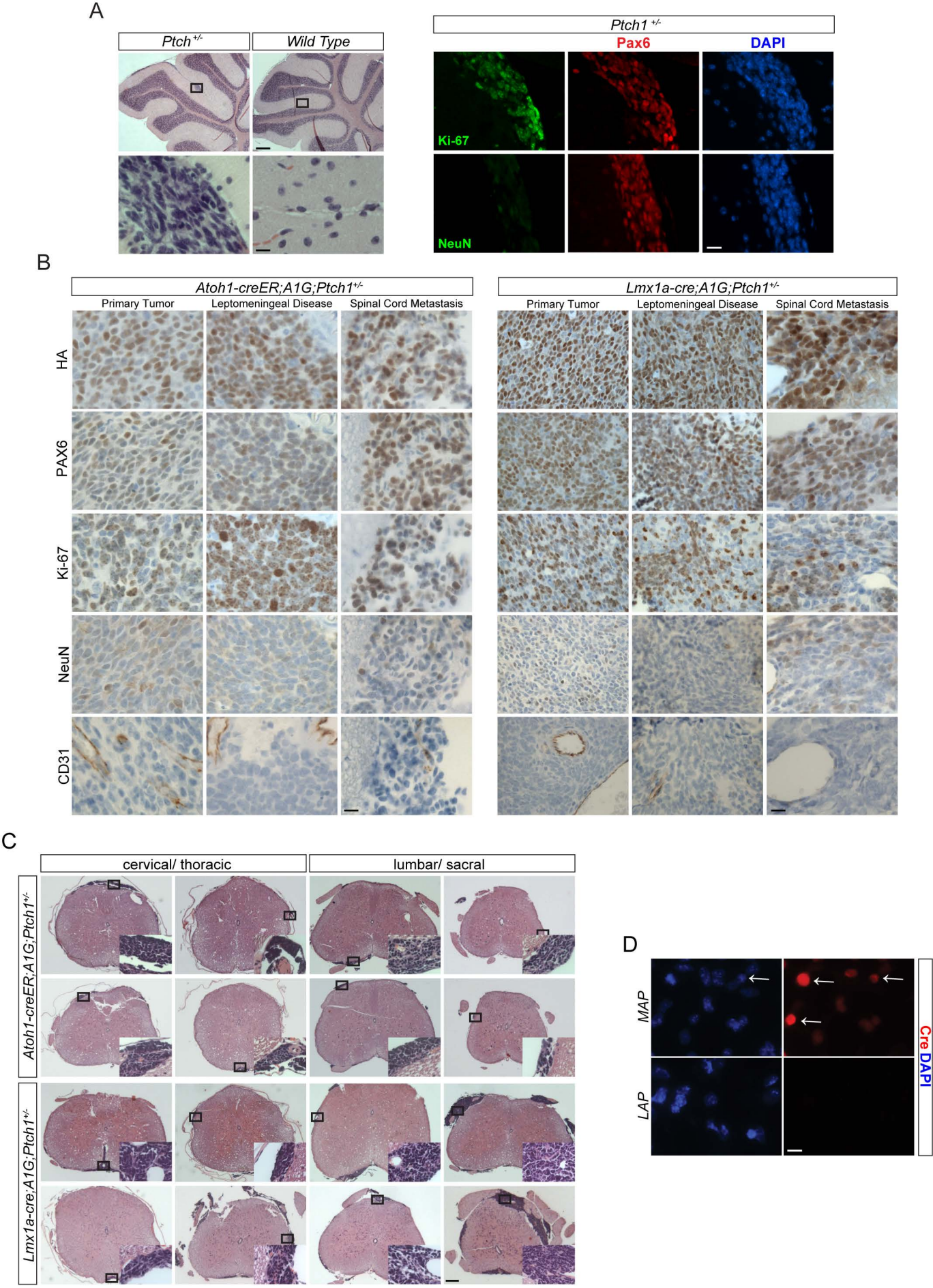

Supplemental figure 6

Supplemental Figure 6 ATOH1-driven development and metastasis in *AAP* and *LAP* mice. (A) H&E staining of cerebellum in *Ptch1*$^{+/-}$ and wild type (WT) mice at 6 weeks of age (left panel). Boxed regions in representative images are magnified in bottom row (left panel). The expression of PAX6 (red), Ki-67 (red), and NeuN (red) is shown in pre-neoplastic cells in representative *Ptch1*$^{+/-}$ mice (right panel). Scale bars, 250 μm (top row) and 12.5 μm (bottom rows). (B) The expression of ATOH1-HA, PAX6, Ki- 67, NeuN, and endothelial marker CD31 is shown cells in primary tumor, leptomeningeal space, and spinal metastatic tumor in representative tamoxifen-treated *Atoh1-creER;A1G;Ptch1*$^{+/-}$ (*AAP*, left panel) animals and *Lmx1a-cre;A1G;Ptch1*$^{+/-}$ (*LAP*, right panel) animals. Scale bars, 12.5 μm. (C) H&E staining is shown for metastatic tumor at different levels of the spinal cord in tamoxifen-treated *AAP* mice and *LAP* mice. Boxed regions in representative images are magnified in inset pictures. Notice that metastatic tumor extends along the entire spinal cord in these mice as observed in *MAP* mice (Supplemental Figure 3, B and C). Scale bar, 250 μm. (D) Representative image of Cre (red) expression is shown in cultured tumor cells. Arrows mark tumor cells from *MAP* mice expressing Cre. Notice that Cre expression is absent in tumor cells from *LAP* animals. DAPI staining (blue) labels nuclei. Scale bar, 5 μm.

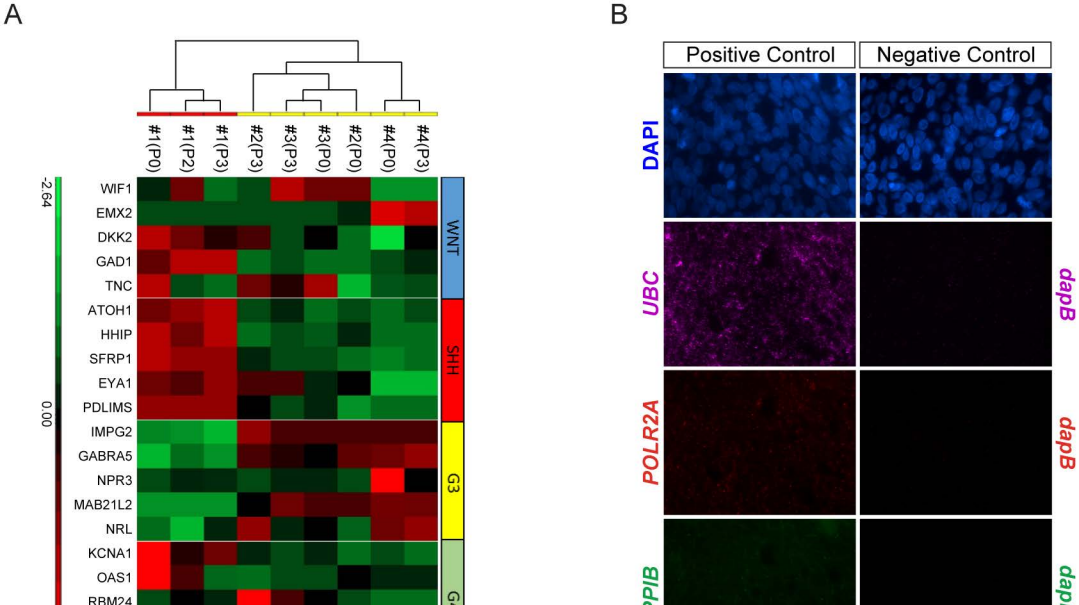

Supplemental figure 7

Supplemental Figure 7 Analysis of gene expression in human MB. (A) NanoString analysis of mRNA extracted from primary MB of patients (#1 - #4) and matched PDX after variable passages (P0 - P3) in recipient animals. Notice that PDXs retain gene expression signature of primary tumors after multiple passages. (B) Representative images are shown for RNAscope multiplex fluorescence analysis of gene expression in SHH MB in humans. Samples were stained for the expression of housekeeping genes *UBC* (Ubiquitin C, magenta), *POLR2A* (DNA-directed RNA polymerase II polypeptide A, red) and *PPIB* (Peptidylprolyl Isomerase B, Cyclophilin B, green) as positive controls. Expression of dapB (dihydrodipicolinate reductase gene from B. subtilis) was used as negative control. DAPI staining (blue) labels nuclei. Scale bar, 5 μm.

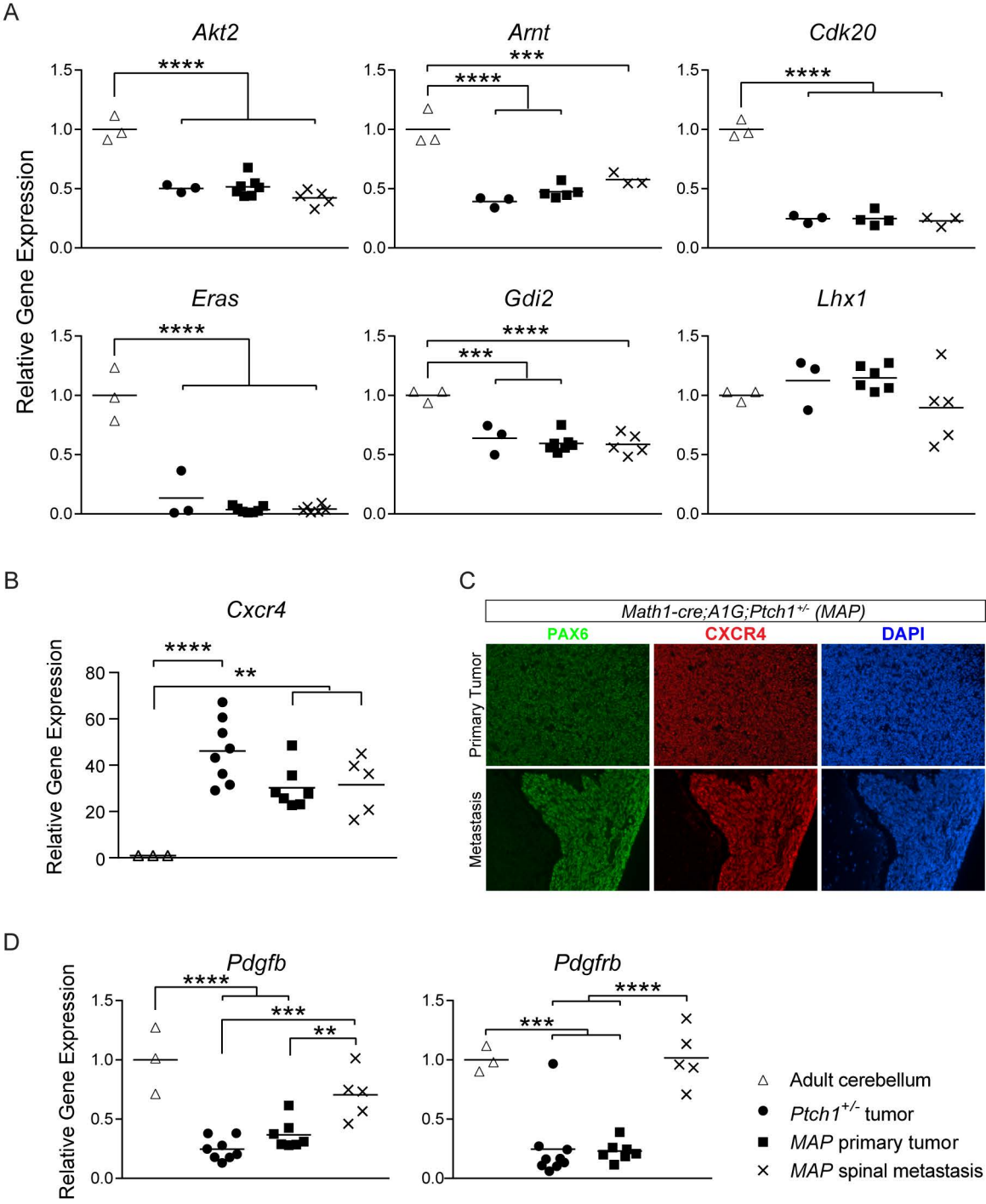

Supplemental figure 8

Supplemental Figure 8 Analysis of gene expression in MB from *MAP* animals. (A) RT-qPCR analysis of gene expression in primary tumor from *MAP* mice (square, *n*=7 tumors from 7 animals for *Akt2, Eras,* and *Gdi2*; *n*=6 tumors from 6 animals for *Lhx1*; *n*=5 tumors from 5 animals for *Arnt*; *n*=4 tumors from 4 animals for *Cdk20*), spinal metastatic tumor from *MAP* mice (x mark, *n*=6 tumors from 6 animals for *Eras*; *n*=5 tumors from 5 animals for *Akt2*, Gdi2, and *Lhx1*; *n*=3 tumors from 3 animals for *Arnt* and *Cdk20*), tumor from *Ptch1*$^{+/-}$ mice (circle, *n*=3 tumors from 3 animals), and in adult wild type cerebellum (triangle, *n*=3 cerebella from 3 animals, data from a single experiment are shown; mean, one-way ANOVA, ****P* <0.001; *****P* <0.0001). (B) RT-qPCR analysis *Cxcr4* expression in primary tumor (square, *n*=4 tumors from 4 animals), spinal metastatic tumor from *MAP* mice (x mark, *n*=3 tumors from 3 animals), tumor from *Ptch1*$^{+/-}$ mice (circle, *n*=3 tumors from 3 animals), and adult wild type cerebellum (triangle, *n*=3 cerebella from 3 animals, data from a single experiment are shown; mean, one-way ANOVA, ***P* <0.01; ****P* <0.001; *****P* <0.0001). (C) Expression of PAX6 (green) and CXCR4 (red) is shown in primary and spinal metastatic tumor in a representative *MAP* mouse. DAPI staining (blue) labels nuclei. Scale bar, 25 μm. (D) RT-qPCR analysis of the expression of *Pdgfb* and *Pdgfrb* in primary tumor (square, *n*=7 tumors from 7 animals), spinal metastatic tumor from *MAP* mice (x mark, *n*=5 tumors from 5 animals), tumor from *Ptch1*$^{+/-}$ mice (circle, *n*=8 tumors from 8 animals), and adult wild type cerebellum (triangle, *n*=3 cerebella from 3 animals, data from a single experiment are shown; mean, one-way ANOVA, ***P* <0.01; ****P* <0.001; *****P* <0.0001).